Original Article
Inhibition of the TGF-β/Smads signaling pathway attenuates pulmonary fibrosis and induces anti-proliferative effect on synovial fibroblasts in rheumatoid arthritis

Shaoqiong Wang, Shuang Wang, Hongbo Li, Lijuan Zhu, Yinghang Wang

Department of Rheumatology, Affiliated Hospital of Changchun University of Traditional Chinese Medicine, Changchun, Jilin Province, P. R. China

Abstract: We explored whether transforming growth factor (TGF-β)/Smads signaling pathway influences rheumatoid arthritis (RA)-associated pulmonary fibrosis (PF) and proliferation of RA synovial fibroblast (RA-SF). Expression levels of TGF-β1 in RA + PF patients, RA patients and healthy controls were determined. Rat models of RA were successfully induced and assigned into groups. The mRNA, phosphorylation and protein expressions of TGF-β1, Smad2 and Smad3 were detected. The serum expressions of inflammatory factors were measured by ELISA. Tissue sections were observed using hematoxylin-eosin (HE) and Masson staining. The SF cells were separated and grouped. Cell viability and migration were determined. The highest expressions of TGF-β1 were found in RA + PF patients, followed by RA patients and then healthy controls. RA + PF rats were characterized by less activity, worse appetite, messy and less shining hair, thin sloppy stool and increased joint swelling. Compared with the normal group, the expressions of TGF-β1, Smad2, Smad3, IL-6 and TNF-α were elevated in the RA + PF group. Meanwhile, the swelling and pulmonary fibrosis of lung tissues was worse, the lung capacity and serum level of IL-10 were decreased. However, SB431542 can reverse the above results. The cell activity and cell migration ability of cells in the RA + PF + SB431542 group were inhibited compared to those in the blank group. Based on above findings, the inhibition of the TGF-β/Smads signaling pathway alleviates the pulmonary fibrosis in rats with RA and suppresses cell viability and migration of synovial fibroblasts.

Keywords: TGF-β/Smads, rheumatoid arthritis, pulmonary fibrosis, synovial fibroblast, migration, SB431542

Introduction

Rheumatoid arthritis (RA) is a chronic auto-immune disorder with a poorly understood etiology [1]. Data has been revealed that the prevalence of RA is approximately 0.5%-1.1% in the developed countries, and a lower incidence rate has been reported in the southern Europe [2]. RA typically manifests with signs of inflammation and characterized by swollen joints, as well as pain and stiffness in joints, particularly stiffness early in the morning when waking or following prolonged inactivity [3]. Even worse, RA may affect other parts of the body, resulting in inflammation around the lung [4]. Lung disease is an extra-articular manifestation (EAM) of RA and the second commonest cause of RA mortality, and it was believed to be either in-volved in the drug therapy for RA, or related to RA comorbid conditions [5]. In addition, synovial fibroblast (SF) also plays a vital role in generating cytokines that facilitate inflammation and proteases contributing to cartilage destruction in RA [6]. In spite of the fact that the precise etiology of RA remains to be explored, both genetic and environmental factors were believed to be involved [7, 8]. Accordingly, the investigations on the pathological mechanism of RA in a genetic approach are needed.

Ligands of the transforming growth factor β superfamily, like transforming growth factor β (TGF-β), have been demonstrated to control the development process of cells through regulating cell proliferation, survival, differentiation and migration [9]. The abnormal activity of the

TGF-β signaling pathway has been suggested to be associated with several human diseases, including malignant tumors, cardiovascular diseases and fibrotic diseases [10]. Additionally, TGF-β signaling activities interact with Smad mediators to mediate multiple biological processes [11]. Interestingly, TGF-β1, by activating its downstream Smad signaling pathway, was proved as a key regulator in renal fibrosis [12]. Moreover, in rats with cardiac fibrosis, suppression of the TGF-β1/Smad3 signaling pathway by metformin causes significant declines in cardiac fibrosis in rat models [13]. The present study aims to explore the effect of the TGF-β/Smads signaling pathway in RA + PF and proliferation of RA synovial fibroblast (RA-SF), by establishing rat models of RA and RA + PF and determining the expression of TGF-β/Smads signaling pathway-related proteins.

Materials and methods

Subjects

From April 2015 to April 2017, 98 RA patients admitted to Affiliated Hospital of Changchun University of Traditional Chinese Medicine were included in the current study, among which 48 patients (25 males and 23 females) were complicated with PF (short for RA + PF) with a mean age of 52.8 ± 17.6 years, and 50 patients (26 males and 24 females) had merely RA with a mean age of 53.4 ± 18.1 years. Meanwhile, another 52 healthy controls who underwent physical examination in our hospital were recruited as control group, including 24 females and 28 males with a mean age of 51.7 ± 16.9 years. The blood sample from patients with empty stomach was collected for further usage. This study was conducted based on the protocols approved by the Ethics Committee. All patients signed written informed consents prior to the study. 2 RA patients admitted to our hospital for knee arthroplasty were included in this study, who were diagnosed based on the diagnostic criteria for RA proposed by American College of Rheumatology (ACR) in 1987. The synovial tissues from each patient were obtained with prior approval from the patients and their chief doctors.

Animal grouping and treatment

Clean staged healthy SD rats (n = 120, half male and half female) with a mean weight of

200 ± 20 g were purchased from the Experimental Animal Center of the Third Military Medical University (license no.: SCXK (YU) 2007-0005, Chongqing, China). Rats were fed for one week for adaption with circadian rhythm and free access to food and water in clean staged animal rooms at room temperature of 22-25°C. After that, rats were assigned into five groups, each group with 24 rats, namely normal group (normal rats without any treatment), negative control group (NC group, rats injected with the same volume of normal saline), RA group (RA rats), RA + PF group and RA + PF + SB431542 group. The RA models were established in both the RA + PF group and the RA + PF + SB431542 group. Following model establishment, rats were anesthetized by injecting 3% pentobarbital sodium (30 mg/kg) in the abdominal cavity. Then the windpipe in the neck was cut open and exposed under sterilized conditions. The bleomycin A5 (5 mg·kg^{-1}, Taihe Pharmaceutical Co., Ltd., Guiyang, Guizhou, China) which was diluted in 0.2 ml of normal saline was injected in the windpipe top to induce PF once RA models were successfully established on 28th day during modeling. The rats were immediately lifted up in the NC, RA + PF and RA + PF + SB431542 groups to allow the medication to fully spread to the lung. At the 3rd, 4th and 5th day after model establishment, rats in the RA + PF + SB431542 group were injected with 0.5 g/L of SB431542 solution in the abdominal cavity (Sigma Aldrich, St. Louis, MO, USA, 4.2 mg/Kg, diluted in 10% of ethanol). Rats in the RA + PF group were injected with the same volume of 10% ethanol. Then on the 7th, 14th and 28th day, 8 rats were randomly selected in each group for further experiment. Animal experiments were conducted in strict accordance with the approved animal protocols and guidelines established by Medicine Ethics Review Committee for animal experiments of our hospital. All efforts were made to minimize the suffering of animals.

Establishment and identification of RA rat models

CCII (Sigma Aldrich, St. Louis, MO, USA) diluted in 0.1 mol/L glacial acetic acid (Sinopharm Chemical Reagent Co., Ltd, Shanghai, China) and complete Freund's adjuvant (CFA, Sigma Aldrich, St. Louis, MO, USA) of the same volume were sufficiently emulsified into the solution with final concentration of 0.5 g/L. Then rats

were anesthetized using 3% pentobarbital sodium (30 mg/kg, Shanghai Zhanyun Chemical Co., Ltd., Shanghai, China), followed by respective subcutaneous injection of 1 mL of type II collagen solution under their back and tail end. The injection of type II collagen solution was performed one week later with the same approach and the same volume, and the rats in the NC group were injected with the same volume of normal saline. On 0, 7th, 14th, and 28th during modeling, the physical activity, fur color, excrement, weight and appetite of normal and modeled rats were observed and recorded. The joint swelling and toe volume were also measured using a joint volume measurer. On 28th day during RA modeling, the DR-X ray films reflecting the joint changes were used to evaluate whether RA models were successfully established.

Preparation of lung tissue samples

Under anesthesia, rats were collected with 3 ml of blood in the heart after their chests were cut open under sterile conditions. Then the blood samples were centrifuged at 3000×g at 4°C for 10 min (centrifugal radius of 15 cm) for serum collection. After that, the serum was stored in a refrigerator at -20°C for further detection of inflammatory factors. Finally, the rats were sacrificed by bloodletting on the carotid artery and their lung tissues in the right chest were obtained and maintained at -70°C of liquid nitrogen. The right lung tissues were stored for reverse transcription quantitative polymerase chain reaction (RT-qPCR) and Western blotting. The left lung was injected with 0.1 mol/L of neutral buffered formalin through the main bronchus to fully unfold the pleura for at least 30 h, followed by embedding in paraffin for hematoxylin-eosin (HE) and Masson staining.

HE staining for pathomorphological changes

The de-waxed sections were immersed in hematoxylin solution for 8 min, followed by washing in double distilled water for 1 min. After dissimilation using 1% of hydrochloric acid ethanol for 8 s and washing in double distilled water for 1 min, the sections were soaked in 1% dilute ammonia for 30 s to turn blue. After another wash in double distilled water for 1 min, the sections were stained by 0.5% eosin solution for 2 min. Then 95% ethanol I and II were used for dehydration with 2 min each time, followed by absolute ethanol I and II for 2 min respectively. The sections were cleared using xylene I, II and III for 2 min respectively. Neutral resins were added in the section which was then sealed using a cover slide for mounting. The pathomorphological changes of lung tissues were observed under a light microscope.

Masson staining for pulmonary fibrosis

Masson staining kit (Nanjing Jiancheng Bioengineering Institute, Nanjing, Jiangsu, China) was used for Masson staining according to the manufacturers' instructions. Prior to the staining, the de-waxed sections were placed in the distilled water for 30-60 s to prevent the sections from drying. Then R1 solution was added in the sections to stain for 4 min. Then the staining solution in the glass slide was removed and the R5 solution was added to rinse the sections for about 30 s. Following that, the R2 solution was dripped to stain for 30 s. Then the staining solution in the glass slide was removed and the R5 solution was added to wash the sections for about 30 s. Subsequently, R3 solution was applied for color development for 7 min, and R4 solution for counterstaining for 3 min, followed by disposal of the R4 solution. Sections were washed in absolute ethanol, dried, and fixed using neutral balsam. The staining of each section was observed under a light microscope, in which the nucleus was dark blue, collagenous fiber, cartilage and grume were blue, and muscle fiber, cellulose and red cells were red. The pulmonary fibrosis was assessed based on following criteria [14]: score 0, no fibrosis; score 1, mild fibrosis, less than 20% of the whole lung; score 2, moderate fibrosis, more than 20% of the whole lung but less than 50%; score 3, serious fibrosis, damaged alveolar structure and formation of pulmonary interstitium scar, more than 50% of the whole lung.

RT-qPCR

Trizol method was applied to extract RNA from samples of blood and lung tissues, which were then identified by ultraviolet analysis and electrophoresis of RNA on gel containing formaldehyde. RNA (1 μg) was then reversely transcribed into cDNA using avian myeloblastosis virus (AMV). PCR primers were designed and synthesized by Invitrogen (Carlsbad, CA, USA) (**Table 1**). Glyceraldehyde-3-phosphate dehydrogenase (GAPDH) was used as an internal control.

Table 1. Primer sequences of TGF-β1, Smad2, and Smad3 used in reverse transcription quantitative polymerase chain reaction (RT-qPCR)

Gene	Sequence
TGF-β1	F: 5'-CTATCACCTACCTTTCCTTGGGAGACC-3'
	R: 5'-GGTAGAGTTCTACGTGTTGCTCCAC-3'
Smad2	F: 5'-AGCCCGTCGGAAGAGGAAGGAAC-3'
	R: 5'-ACTGGCGGAGTGAATGGCAAGAT-3'
Smad3	F: 5'-GAAGTCCTCGGAACTGCCTACCT-3'
	R: 5'-CACCTGATGGCTTTACTGCTACA-3'
GAPDH	F: 5'-CTAAGGCCAACCGTGAAAAG-3'
	R: 5'-ACCAGAGGCATACAGGGACA-3'

Note: F, forward; R, reverse.

The amplification was conducted based on following conditions: 94°C pre-degeneration for 5 min, 94°C degeneration for 40 s, 60°C annealing for 40 s, 72°C extension for 1 min, which ran a total of 40 cycles, followed by 72°C extension for 10 min. PCR product was treated with electrophoresis of agarose gel. Opticon Monitor 3 software (Bio-Rad, Hercules, CA, USA) was used for PCR analysis. The lowest point in the logarithmic amplification curve was manually set to calculate the threshold cycle (Ct) value. Data were analyzed using the $2^{-\triangle\triangle Ct}$ method.

Western blotting

The frozen lung tissues stored in liquid nitrogen was collected and placed on the ice. The tissues (200 mg) were extracted with 200 μl phosphate-buffered saline (PBS). A bicinchoninic acid (BCA) kit (Wuhan Boster Biological Technology Co., Ltd., Wuhan, Hubei, China) was used to determine the concentration of separate proteins in lung tissues. The voltage of electrophoresis was turned from 80 V to 120 V with wet transfer at 100 mV for 45-70 min. The rabbit anti-rat antibodies of TGF-β1, Smad2/Smad3 and p-Smad2/Smad3 (diluted at 1:1000, Cell Signaling Technology, Boston, MA, USA), as well as anti-rat primary antibody of β-actin (diluted at 1:3000, Becton Dickinson, Mountain View, CA, USA) were added and incubated at 4°C overnight. Corresponding secondary antibodies (Shanghai MT-bio, Shanghai, China) were supplemented for incubation at room temperature for 1 h. The images of the gels were captured in a Bio-Rad Gel Doc EZ Imager (Bio-Rad, Hercules, CA, USA), and the grey value of target band was analyzed using ImageJ software.

Enzyme-linked immunosorbent assay (ELISA)

ELISA was applied to detect the expression of TGF-β1, interleukin-6 (IL-6), IL-10 and tumor necrosis factor-α (TNF-α). Based on the instructions of ELISA kit, the separated serum levels of TGF-β1 (31-2000 pg/ml, catalog no: BMS-24904), IL-6 (3.1-200 pg/ml, catalog no: BM-S213-2), IL-10 (2-300 pg/ml, catalog no: KH-C0101) and TNF-α (15.6-1000 pg/ml, catalog no: BMS223HS) (Invitrogen, Carlsbad, CA, USA) were measured.

Cell isolation and culture

A total of 2 RA patients admitted in our hospital for knee arthroplasty were included in this study, who were diagnosed on the basis of the diagnostic criteria for RA proposed by American College of Rheumatology (ACR) in 1987. The synovial tissues from each patient were obtained with prior approval from the patients and their chief doctors. After removal of the adipose tissues and large vessels, the synovial tissues were washed in normal saline for three times to remove the blood and impurities. Then, the synovial tissues were sliced into pieces of 1 mm³, which were then transferred in to a culture flask with a pipette. Then a 2 mL syringe needle was used to arrange the tissue samples with an interval of 5 mm. The culture flask was overturned to add culture medium in the flask on the other side without tissues covering. Tissue samples were then incubated in an incubator at 37°C for 4 h with 5% CO_2. To maximum the contact of tissues to culture medium, the culture flask was overturned again. Culture medium was replaced once after cells were incubated for 2-5 days. Cells were then subcultured after cell confluence reached 70%. The sub-cultured cells were digested with culture medium containing 1 mL of 0.25% trypsin. The cell culture was terminated when cells shrunk and turned round. Then the cell suspension was cultured at a ratio of 1:2 in separate flasks to obtain the 3rd~5th generated cells. Cell morphology and cell growth were observed under an inverted microscope.

Cell identification and grouping

The isolated cells were identified using Vimentin and CD68 immunocytochemical staining. The 3rd~6th generated cells were digested and resuspended into 1×10⁵ cells/mL single cell

suspension, which was then inoculated in a 48-well plate for cell culture. Twenty-four hours later, cells were fixed with 4% paraformaldehyde for 20 min, followed by washing in PBS for 3 times (5 min each time). Then the cells were treated with Tritonx-100 for 20 min. After that, 3% H_2O_2 was added and incubated for 15 min, followed by blocking with goat serum at 37°C for 30 min. Subsequently, the goat serum was discarded and the primary antibody (1:100) was added at 4°C for overnight. The negative control for the primary antibody was PBS. After cells were washed in PBS for 3 times (5 min each time), secondary antibody (solution B) was added for incubation at 37°C for 20 min. The PBS wash was repeated, and cells were added with solution C at 37°C and maintained for 20 min. PBS wash was conducted again and diaminobenzidine (DAB) was used for color development for 10 min. The cells were counterstained with hematoxylin. After 80 s, PBS wash was conducted, and cells were sealed with glycerinum buffer. Cells were then observed under a microscope and photographed. Under the microscope, the cytoplasm of the positive cells was brown yellow and nucleus was purple blue, while the nucleus of the negative cells was blue and cytoplasm was colorless. The RA-SF at logarithmic growth phase was grouped into blank group (no treatment), NC group (treated with PBS solution) and SB431542 group (treated with TGF-β/Smads signaling pathway inhibitor SB431542).

MTT assay

Cell suspension was diluted and inoculated in a 96 well plate with a density of $5×10^4$ cells per well. Each group contained 6 parallel wells. After cell confluence reached 80%, cells were grouped and treated separately. Once the reoxygenation was completed, 20 μl of MTT solution (Sigma Aldrich, St. Louis, MO, USA) was added followed by incubation at 37°C. MTT solution was discarded 4 h later. Then cell suspension in each well was added with 150 μl of dimethyl sulfoxide (Sigma Aldrich, St. Louis, MO, USA) and was put on the shaker for 10 min. The optical density (OD) value of each well was measured using a microplate reader with a wavelength of 490 nm. Experiments were conducted for three times to obtain the mean value. Cell survival rate = (OD value of experiment group - OD value of blank group)/OD value of blank group.

Scratch testing

A marker pen was used to draw vertical lines in the back of the 6-well plate. The vertical lines were drawn through the well with an interval of 0.8 cm and each well shall have at least five lines. After that, each well was inoculated with $5×10^5$ cells with cell confluence reaching 100%. On the next day, a 10 μl pipette tip was used to draw a line which was vertical to the line in the back. PBS was then used to wash cells for three times to remove the detached cells. The well plate was added with culture medium in an incubator at 37°C with 5% CO_2. Cell migration ability was assessed, and photos were taken at time points of 0 h, 24 h and 48 h. Experiments were conducted for three times to obtain the mean value.

Statistical analysis

The software SPSS 21.0 (IBM Corp, Armonk, NY, USA) was employed for data analysis. Data were presented by mean ± standard deviation (x ± SD). The pairwise comparison was conducted by the least significant difference and comparison among multiple groups was conducted using one-way analysis of variance (ANOVA). Measurement data complying with the normal distribution were pair-wisely compared using *t* test. *P* value of 0.05 was considered as the critical value for statistical significance.

Results

RA + PF patients had higher serum levels of TGF-β1 than RA patients and healthy controls

ELISA was used to detect the serum levels of TGF-β1 in healthy controls, RA patients and RA + PF patients. RA + PF patients had the higher serum levels of TGF-β1 (451.5 ± 121.3) than those in healthy controls (141.7 ± 42.6) and RA patients (321.7 ± 108.2) (*P* < 0.05). The RA patients had elevated serum levels of TGF-β1 when compared with those in healthy controls (*P* < 0.05).

General characteristics of rats before and after RA modeling

The rats in the normal and NC groups showed normal appetite and water consumption, as well as hair shining and activity, while the weight gradually increased. The rats in the RA + PF group demonstrated less activity, decreased
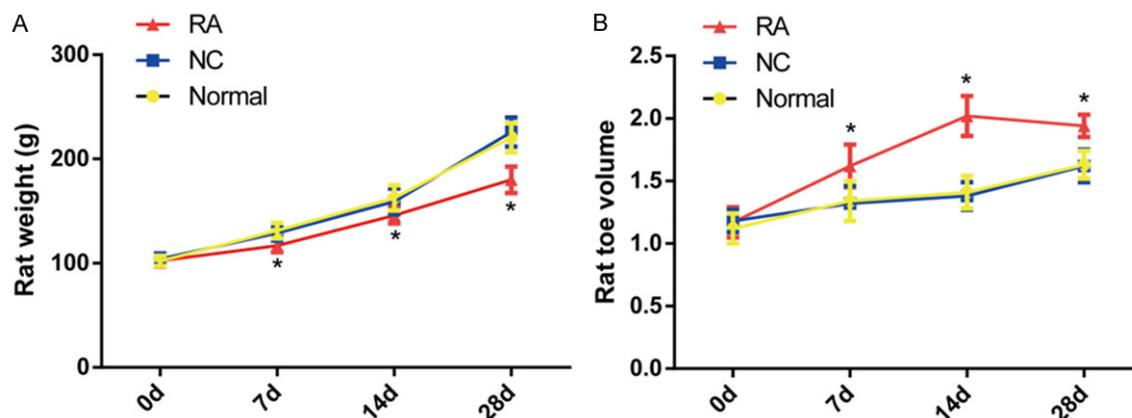
Figure 1. Rat weight and toe volume among groups. Note: (A) Rat weight among normal, NC, and RA groups before and after modeling (g); (B) Rat toe volume among normal, NC, and RA groups before and after modeling. *, $P < 0.05$, compared with the normal group at the same time point; NC, negative control; RA, rheumatoid arthritis.

appetite, less and messy hair, hair removal and thin sloppy stool. The weight of rats in the RA + PF group significantly decreased at 7th day. The difference in weight between rats in the RA + PF group at 14th day and 28th day and those in the normal and NC groups were significantly facilitated (**Figure 1A**). The rats in the RA + PF group showed joint swelling at 7th day; the swelling spread all around the joint with locally ulcerated skin in the joint and rats could hardly walk at 14th day. After 14 days, rats of the RA + PF group exhibited slightly alleviated joint swelling, but still showed obvious difference from those in the normal and NC groups. The toe volume of rats in the RA + PF group at 7th day, 14th day and 28th day were all significantly higher than those in the normal and NC groups (all $P < 0.05$) (**Figure 1B**).

Pathological changes in lung tissues identified under a light microscope

As for rats in the RA + PF group, pulmonary alveolitis was noticeable on the 7th day, which was slightly alleviated on the 14th day but decreased on the 28th day. Infiltration in the alveolus pulmonis was serous and the wall of alveolus pulmonis was thickened. The pulmonary alveolitis was incomplete and the wall of alveolus pulmonis was thickened with infiltration on the 14th day. The pulmonary alveolitis on the 28th day was destructed and missed which resulted in the formation of air cavity, and the fibroplasia was serious with visible collagenous fiber around the air passages and walls of pulmonary alveolitis in strip or flake shape. In addition, the fibroplasia and blue stained collagen

matrix were also observed on the 7th day and 14th day (**Figure 2** and **Table 2**).

Inhibition of the TGF-β/Smads pathway decreased mRNA, protein and phosphorylation levels of TGF-β1, Smad2 and Smad3 in RA + PF rats

Compared with the normal group, the mRNA, protein and phosphorylation levels of TGF-β1, Smad2 and Smad3 in the NC group were not significantly different (all $P > 0.05$), while those in the RA group, RA + PF group and RA + PF + SB31542 group were elevated. It is indicated that RA + PF group had the highest mRNA, protein and phosphorylation levels of TGF-β1, Smad2 and Smad3, followed by RA + PF + SB431542 group (all $P < 0.05$) (**Figure 2**).

Inhibition of the TGF-β/Smads pathway resulted in decreased IL-6 and TNF-α levels, but increased IL-10 level

The serum levels of IL-6 and TNF-α were increased, and the serum level of IL-10 was decreased in the RA group when compared with those in the normal group (all $P < 0.05$). The RA + PF group had increased serum levels of IL-6 and TNF-α, and further decreased serum level of IL-10, when compared with those in the normal group and the RA group (all $P < 0.05$). The results showed that, in rats of the RA + PF + SB431542 group, where the TGF-β/Smads signaling pathway was inhibited by SB431542, the serum levels of IL-6 and TNF-α were decreased, but the serum level of IL-10 was increased (all $P < 0.05$) (**Table 3**).
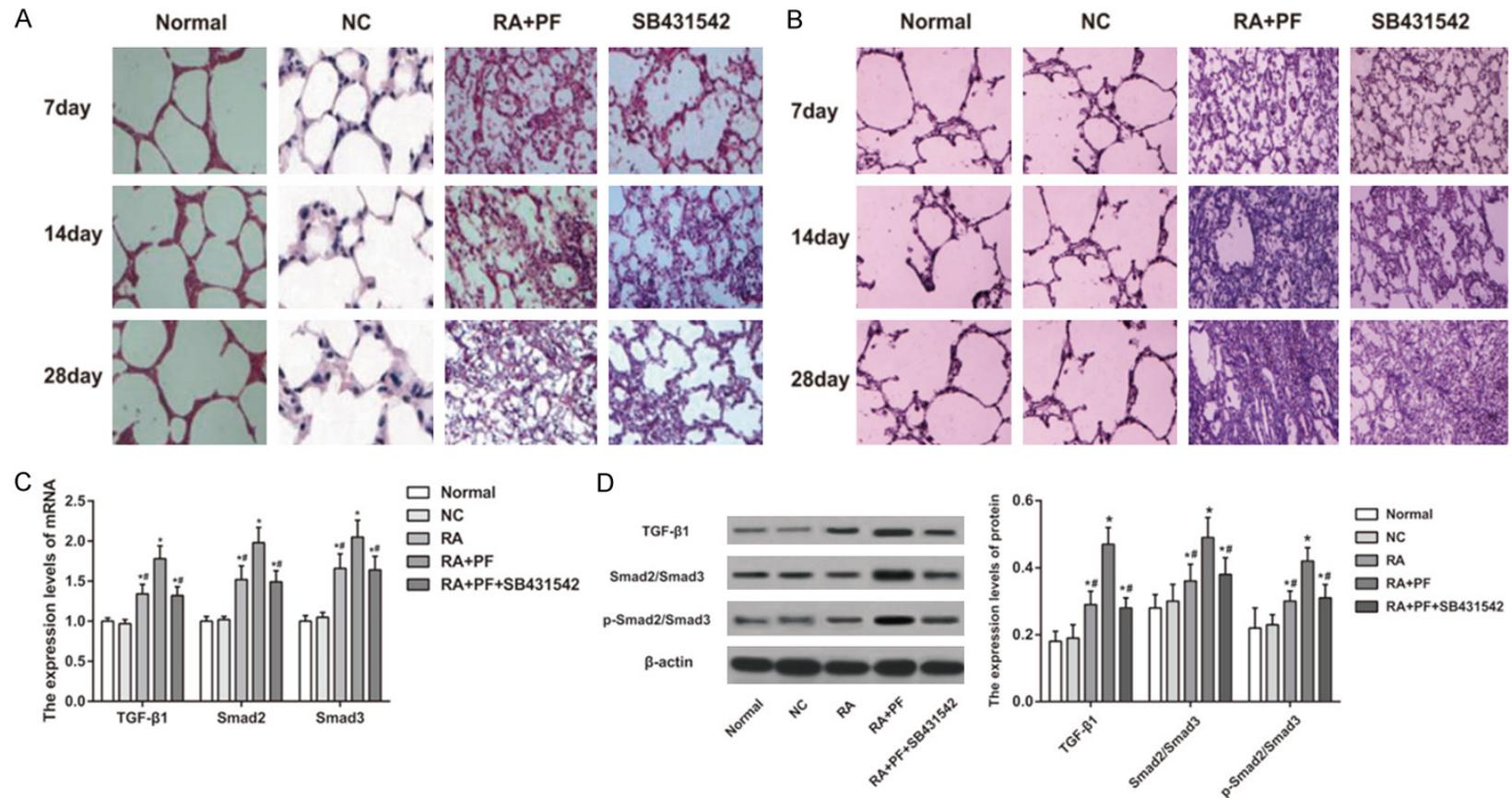
Figure 2. Pathological changes and expression levels of TGF-β1, Smad2 and Smad3 in rat lung tissues. Note: (A) HE staining (×400); (B) Masson staining (×400); (C) mRNA expressions of TGF-β1, Smad2 and Smad3; (D) Protein expressions of TGF-β1, Smad2/Smad3 and p-Smad2/Smad3; *, $P < 0.05$ compared with the normal group; #, $P < 0.05$ compared with the RA + PF group; HE, hematoxylin-eosin; RA, rheumatoid arthritis; NC, negative control; PF, pulmonary fibrosis.

Table 2. Pulmonary alveolitis and pulmonary fibrosis in lung tissues of rats among normal, NC, RA, RA + PF, and RA + PF + SB431542 groups 7, 14 and 28 days after modeling

Group	Pulmonary alveolitis			Pulmonary fibrosis		
	7 d	14 d	28 d	7 d	14 d	28 d
Normal group	0.00 ± 0.00	0.00 ± 0.00	0.00 ± 0.00	0.00 ± 0.00	0.00 ± 0.00	0.00 ± 0.00
NC group	0.00 ± 0.00	0.00 ± 0.00	0.00 ± 0.00	0.00 ± 0.00	0.00 ± 0.00	0.00 ± 0.00
RA group	1.68 ± 0.31*	1.47 ± 0.25*	0.58 ± 0.14*	0.32 ± 0.07*	1.01 ± 0.16*	1.39 ± 0.28*
RA + PF group	2.35 ± 0.47	2.02 ± 0.41	1.28 ± 0.26	0.65 ± 0.11	1.67 ± 0.32	2.14 ± 0.43
RA + PF + SB431542 group	1.74 ± 0.32*	1.42 ± 0.23*	0.61 ± 0.12*	0.35 ± 0.08*	0.98 ± 0.19*	1.43 ± 0.27*

Note: *, $P < 0.05$, compared with the RA + PF group at the same time point; NC, negative control; RA, rheumatoid arthritis; PF, pulmonary fibrosis.

Table 3. Serum levels of inflammatory factors (IL-6, TNF-α and IL-10) in rats among normal, NC, RA, RA + PF, and RA + PF + SB431542 groups (pg/ml)

Group	IL-6	IL-10	TNF-α
Normal group	49.62 ± 5.03	56.25 ± 5.67	90.24 ± 8.02
NC group	48.79 ± 5.14	54.32 ± 5.81	89.53 ± 8.11
RA group	69.18 ± 6.07*,#	27.35 ± 2.98*,#	139.84 ± 9.35*,#
RA + PF group	89.46 ± 7.25*	13.16 ± 1.43*	178.65 ± 9.89*
RA + PF + SB431542 group	68.35 ± 6.11*,#	28.21 ± 3.09*,#	137.92 ± 9.76*,#

Note: *, $P < 0.05$ compared with the normal group; #, $P < 0.05$ compared with the RA group; NC, negative control; RA, rheumatoid arthritis; PF, pulmonary fibrosis; TGF-β1, transforming growth factor β1.

Observation and identification of SF

The cells observed under an inverted microscope were presented in cambiform, star-shaped and fusiform with majority cells in corniform, which conform to the characteristics of SF cells. Cell nucleus was located in the middle of the cell with clear boundary in round and oval shape. The passaged SF cells of the third generation were characterized by disappearance of dendritic cells, endothelial cells, adipose cells and vascular endothelial cells and no suspension cells was found. After cells were passaged for more than the third generation, SF cells took up a proportion of above 98%. Vimentin and CD68 immunocytochemical staining were used to identify SF cells. The SF cells were Vimentin positive, in which large proportion of brown yellow particles were found in SF cells. The CD68 staining showed negative staining in SF cells, which indicated that SF cells were isolated successfully (**Figure 3**).

Inhibition of the TGF-β/Smads pathway suppressed SF cell activities

At 24 h and 48 h, the cell activities in the SB431542 group was significantly decreased when compared with those in the blank and PBS groups, which implied that the inhibition of the TGF-β/Smads pathway suppressed the SF cell activities (**Figure 3**). The migration abilities at 24 h and 48 h in the SB431542 group were repressed, in comparison with those in the blank group and the PBS group (all $P < 0.05$), which suggested that inhibition of the TGF-β/Smads pathway suppressed the migration ability of SF cells (**Figure 3**).

Discussion

In the current study, PF and activities of SF were explored in rat models of RA and RA patients. The effect of the TGF-β/Smads signaling pathway on RA + PF was investigated by measuring the expressions of pathway-related proteins. Our results revealed that the rats with RA + PF were presented with increased expressions of TGF-β1, Smad2 and Smad3, which suggested that the TGF-β/Smads signaling pathway was activated in RA + PF. In contrast, SB-431542 suppressed the expression of the TGF-β/Smads signaling pathway-related proteins, indicating that the activation of signaling pathway was suppressed by this inhibitor. Moreover, PF and proliferation of RA-SF were inhibited in the RA + PF + SB431542 group. Conclusively, the inhibition of the TGF-β/Smads signaling pathway ameliorated PF and inhibited the activity and proliferation of RA-SF in RA.

As the results revealed in our study showed that RA + PF resulted in elevated expressions
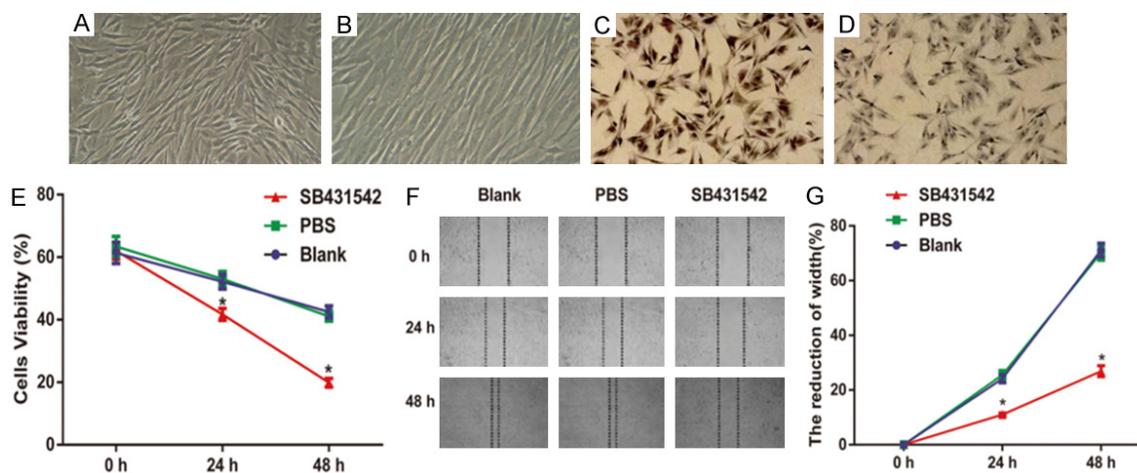
Figure 3. Observation and identification of synovial fibroblasts and cell abilities. A. Images of synovial fibroblasts under an inverted microscope (×100); B. Images of synovial fibroblasts under an inverted microscope (×200); C. Positive Vimentin immunocytochemical staining (×200); D. Negative CD68 immunocytochemical staining (×200); E. Results of cell viability; F. Images of migration ability for each group; G. Statistical analysis of the reduction of scratch width; *, $P < 0.05$ compared with the blank group.

of inflammation factors, including IL-6 and TNF-α. The TGF-β1/Smad signaling pathway was activated during the onset of RA + PF. Inflammation in RA has been previously demonstrated, but the possible association between inflammation and cell response in RA remains undefined, which may be a trigger of the onset of RA [15]. It has been revealed that there may be several signaling pathways of TNF release in the occurrence and development of RA [16]. As joint damages in RA initially happened in the synovial membranes, in which the activation of mononuclear cells and the formation of new blood vessels may result in synovitis, and the secretion of cytokines, especially TNF-α, IL-6 and IL-1, may cause synovial inflammation [1]. Previous study focusing on treatment of RA found that blockade of IL-1 and TNF-α may be beneficial for therapeutic effects on RA [17]. Additionally, PF was characterized by the accumulation of fibroblasts and myofibroblasts, and there were several risk factors that may initiate the onset of it, though most PF arose in nature [18, 19]. One probable mechanism was that acute inflammatory responses were involved in the development of PF. In RA, SFs are major cells contributing to the exacerbation of joint erosion and inflammation [20]. Nevertheless, the exact cellular response and interaction within the micro-environment was still worth our attention for further exploration. Evidence supported that the possible mechanism of regulatory effects on the TGF-β1/Smad signaling

in fibrosis may be attributed to short and long noncoding RNA molecules and epigenetic modifications of DNA and histone proteins [21].

Considering the observation of SF in our study, it suggested that the inhibition of the TGF-β/Smads signaling pathway attenuated SF migration and proliferation abilities. Consistently, fibroblasts play a critical role in immune responses to tissue injuries and it is proved that the fibroblast proliferation may promote the formation of pannus and eventually cause joint destruction in RA [22]. Meanwhile, Smad has been documented to be involved in inflammation. This was evident with the supportive finding that the cardiac inflammation was inhibited in mice with Smad knockdown, suggesting the modulatory role of Smad in cell inflammation of Ang II-induced cardiac inflammation [23]. Therefore, it is possible that the TGF-β/Smads signaling pathway was activated upon the stimulation of Smads to promote the proliferation and migration of fibroblasts in RA, leading to deterioration of RA. However, due to limited sample size and experiment time period, an extended investigation into the promotion effects of the TGF-β/Smads signaling pathway on the progression of RA is required to be conducted in the future.

In summary, observations and findings in the present study supported that the inhibition of the TGF-β/Smads signaling pathway alleviated

PF in association with RA and inhibited the migration and proliferation of SF. This study may provide clinical values for RA treatment as we proposed that TGF-β/Smads signaling pathway may be a therapeutic target for PF associated with RA treatment and suppression of SF proliferation.

Acknowledgements

Disclosure of conflict of interest

None.

Address correspondence to: Dr. Yinghang Wang, Department of Rheumatology, Affiliated Hospital of Changchun University of Traditional Chinese Medicine, 1478 Gongnong Road, Changchun 130021, Jilin Province, P. R. China. Tel: +86-0431-86178018; E-mail: wangyinghang08@163.com

References

[1] Boissier MC, Semerano L, Challal S, Saidenberg-Kermanac'h N and Falgarone G. Rheumatoid arthritis: from autoimmunity to synovitis and joint destruction. J Autoimmun 2012; 39: 222-228.

[2] Tobon GJ, Youinou P and Saraux A. The environment, geo-epidemiology, and autoimmune disease: rheumatoid arthritis. J Autoimmun 2010; 35: 10-14.

[3] Stack RJ, van Tuyl LH, Sloots M, van de Stadt LA, Hoogland W, Maat B, Mallen CD, Tiwana R, Raza K and van Schaardenburg D. Symptom complexes in patients with seropositive arthralgia and in patients newly diagnosed with rheumatoid arthritis: a qualitative exploration of symptom development. Rheumatology (Oxford) 2014; 53: 1646-1653.

[4] Harlow L, Rosas IO, Gochuico BR, Mikuls TR, Dellaripa PF, Oddis CV and Ascherman DP. Identification of citrullinated hsp90 isoforms as novel autoantigens in rheumatoid arthritis-associated interstitial lung disease. Arthritis Rheum 2013; 65: 869-879.

[5] Lake F and Proudman S. Rheumatoid arthritis and lung disease: from mechanisms to a practical approach. Semin Respir Crit Care Med 2014; 35: 222-238.

[6] Bartok B and Firestein GS. Fibroblast-like synoviocytes: key effector cells in rheumatoid arthritis. Immunol Rev 2010; 233: 233-255.

[7] Szodoray P, Szabo Z, Kapitany A, Gyetvai A, Lakos G, Szanto S, Szucs G and Szekanecz Z. Anti-citrullinated protein/peptide autoantibodies in association with genetic and environmental factors as indicators of disease outcome in rheumatoid arthritis. Autoimmun Rev 2010; 9: 140-143.

[8] Liu Y, Aryee MJ, Padyukov L, Fallin MD, Hesselberg E, Runarsson A, Reinius L, Acevedo N, Taub M, Ronninger M, Shchetynsky K, Scheynius A, Kere J, Alfredsson L, Klareskog L, Ekstrom TJ and Feinberg AP. Epigenome-wide association data implicate DNA methylation as an intermediary of genetic risk in rheumatoid arthritis. Nat Biotechnol 2013; 31: 142-147.

[9] Bierie B and Moses HL. Transforming growth factor beta (TGF-beta) and inflammation in cancer. Cytokine Growth Factor Rev 2010; 21: 49-59.

[10] Horbelt D, Denkis A and Knaus P. A portrait of Transforming Growth Factor beta superfamily signalling: background matters. Int J Biochem Cell Biol 2012; 44: 469-474.

[11] Drabsch Y and ten Dijke P. TGF-beta signalling and its role in cancer progression and metastasis. Cancer Metastasis Rev 2012; 31: 553-568.

[12] Lan HY. Diverse roles of TGF-beta/Smads in renal fibrosis and inflammation. Int J Biol Sci 2011; 7: 1056-1067.

[13] Xiao H, Ma X, Feng W, Fu Y, Lu Z, Xu M, Shen Q, Zhu Y and Zhang Y. Metformin attenuates cardiac fibrosis by inhibiting the TGFbeta1-Smad3 signalling pathway. Cardiovasc Res 2010; 87: 504-513.

[14] Szapiel SV, Elson NA, Fulmer JD, Hunninghake GW and Crystal RG. Bleomycin-induced interstitial pulmonary disease in the nude, athymic mouse. Am Rev Respir Dis 1979; 120: 893-899.

[15] Konisti S, Kiriakidis S and Paleolog EM. Hypoxia--a key regulator of angiogenesis and inflammation in rheumatoid arthritis. Nat Rev Rheumatol 2012; 8: 153-162.

[16] Lichtenthaler SF. iRHOM2 takes control of rheumatoid arthritis. J Clin Invest 2013; 123: 560-562.

[17] Gaffen SL. The role of interleukin-17 in the pathogenesis of rheumatoid arthritis. Curr Rheumatol Rep 2009; 11: 365-370.

[18] Biswas R, Bunderson-Schelvan M and Holian A. Potential role of the inflammasome-derived inflammatory cytokines in pulmonary fibrosis. Pulm Med 2011; 2011: 105707.

[19] Pardo A and Selman M. Lung fibroblasts, aging, and idiopathic pulmonary fibrosis. Ann Am Thorac Soc 2016; 13: S417-S421.

[20] Neumann E, Lefevre S, Zimmermann B, Gay S and Muller-Ladner U. Rheumatoid arthritis progression mediated by activated synovial fibroblasts. Trends Mol Med 2010; 16: 458-468.

[21] Meng XM, Nikolic-Paterson DJ and Lan HY. TGF-beta: the master regulator of fibrosis. Nat Rev Nephrol 2016; 12: 325-338.

[22] Wang M, Wu J, Guo Y, Chang X and Cheng T. The tripartite motif-containing protein 3 on the proliferation and cytokine secretion of rheumatoid arthritis fibroblast-like synoviocytes. Mol Med Rep 2017; 15: 1607-1612.

[23] Huang XR, Chung AC, Yang F, Yue W, Deng C, Lau CP, Tse HF and Lan HY. Smad3 mediates cardiac inflammation and fibrosis in angiotensin II-induced hypertensive cardiac remodeling. Hypertension 2010; 55: 1165-1171.